Effects of grain size on the dielectric properties of $Pb(Mg_{1/3}Nb_{2/3})O_3$-30 mol % $PbTiO_3$ ceramics

Wook Jo,[a] Tae-Hyeong Kim, and Doh-Yeon Kim
Department of Materials Science and Engineering, Seoul National University, Seoul 151-744, Korea

Shyamal Kumar Pabi
Metallurgical and Materials Engineering Department, Indian Institute of Technology, Kharagpur, W.B. 721302, India

(Received 6 March 2007; accepted 14 August 2007; published online 12 October 2007)

The effects of the average grain size on the phase transformation and consequent changes in the dielectric properties of $Pb(Mg_{1/3}Nb_{2/3})O_3$-30 mol % $PbTiO_3$ were investigated. It was observed that the size refinement down to ~90 nm impeded the phase transformation of the cubic phase formed in the course of sintering either into rhombohedral or into tetragonal one, and a series of phase transformation from cubic to rhombohedral and then to tetragonal phase took place as the average grain size increased from ~90 nm to ~5.7 μm. This dependence of the crystal structure on the grain size was qualitatively explained in terms of the capillarity effect and the free volume at the grain boundaries exerting a negative hydrostatic pressure on the grains. With the change in crystal structure the typical ferroelectric behavior in dielectric properties evolved into that of a relaxor and finally into a paraelectric one. The overall changes in the dielectric behavior were interpreted on the basis of the size-driven phase transformation. An anomalous dielectric behavior, i.e., a relatively high dielectric constant over a wide range of temperature (30–330 °C), was observed at the average grain size of ~330 nm possibly due to a state of a single domain in a single grain, while below ~90 nm all the phases in the system practically transformed into the paraelectric cubic phase. © *2007 American Institute of Physics*. [DOI: 10.1063/1.2794377]

I. INTRODUCTION

Ultrahigh piezoelectric properties were discovered in the recent past in the ⟨001⟩ oriented rhombohedral $Pb(Mg_{1/3}Nb_{2/3})O_3$-*x* mol % $PbTiO_3$ (PMN-*x*PT) single crystals of near the morphotropic phase boundary (MPB) composition[1] and they were attributed to the polarization rotation, which was induced by the transformation from rhombohedral to tetragonal structure under the influence of an electric field.[1,2] However, the low Curie temperature (T_C) and the rhombohedral to tetragonal phase transformation with a small increase in temperature owing to the presence of undesirable curvature in the MPB composition make practical applications of PMN-PT rather limited.[3] Therefore, the key to make the PMN-30PT system (a rhombohedral-rich MPB composition) appropriate for practical applications should be to increase T_C and extend the stability of the rhombohedral phase to elevated temperatures. This is, of course, not readily achievable, because the transformation from rhombohedral to tetragonal structure in PMN-30PT is normally a function only of the composition and temperature.[3] Recent research activities are therefore directed toward exploring alternative materials with high T_C, such as the $BiScO_3$-$PbTiO_3$ system.[4]

On the other hand, Ramer *et al.*[5] reported that a uniaxial stress along ⟨001⟩ direction can also induce a reversible phase transformation between rhombohedral and tetragonal phase in perovskite-based systems, i.e., when a compressive stress is applied to the tetragonal phase along the *c* axis, the tetragonal phase converts to a rhombohedral one. The result indicates that if a compressive stress could be intrinsically developed in the PMN-PT system at MPB, not only the transformation from the rhombohedral to the tetragonal phase can be suppressed, but also the pre-existing tetragonal phase in MPB composition can be transformed into the preferred rhombohedral phase without any modification to the composition.

A possible way to impose intrinsic stresses on the system would be to reduce the average grain size of the system. The stresses can be inherited not only by a nanocrystalline system from its synthesis route such as a high energy ball milling but also by a negative hydrostatic pressure (NHP) induced by the increase in the free volume at the grain boundaries of the nanostructured bulk materials.[6,7] Besides, the surface bond contraction due to the reduction in ionic radius of the surface atoms is known to cause compressive stresses on the inner part of individual grains and manifest dielectric anomaly.[8,9] Moreover, any change in the specific volume owing to changes in crystal structure may further complicate the stress scenario in polycrystalline aggregates.

A number of investigations in recent times was directed to study the effect of the grain size on the dielectric properties of various ferroelectric materials.[10–24] A consistent result is that the reduction in grain size causes a depression in the Curie temperature and the dielectric constant and finally leads to a system with a single domain in a single grain.[11,14,15,17] While most of the investigations on the nano-

[a]Author to whom correspondence should be addressed. Present address: Institute of Materials Science, University of Technology, D-64287 Darmstadt, Germany. Electronic mail: jo@ceramics.tu-darmstadt.de

structured ferroelectrics in the past were performed on the powder or porous mass, a recent systematic investigation by Zhao *et al.*[12] on the dense nanocrystalline $BaTiO_3$ ceramics has revealed a progressive reduction of the tetragonal distortion, heat of transition, Curie temperature, and relative dielectric constant as the grain size decreases from 1200 to 50 nm. Their results strongly support the existence of an intrinsic size effect in bulk specimens. The critical size for the disappearance of ferroelectricity in their ceramics was evaluated to be 10–30 nm.

However, when it comes to PMN-based ferroelectric materials, studies on the effect of grain size on the ferroelectric phenomena are rather limited. Although Carreaud *et al.*[24] have recently reported the effects of the nanocrystallization of PMN-35PT down to 15 nm on the dielectric properties, the grain-size distribution and stresses in their porous nanostructured specimen can be quite different from those in fully dense nanostructured bulk samples. It may be mentioned that the conventional pressureless sintering process employed by these investigators is ineffective in retaining the nanostructure after full densification of the ceramics.[25]

In the mean time, according to the well-known theory on the ferromagnetic materials, the size refinement is known to result in a specific state of a single domain in a single grain accompanied with a significant increase in the coercivity, when the particle size reaches a few tens of nanometers.[26] Note that the higher the coercivity is, the higher the spontaneous polarization is. Considering the similarities between ferromagnetism and ferroelectricity, a high level of size refinement even in the ferroelectric materials may result in a useful dielectric material in spite of a certain level of reduction in the dielectric properties, if the state of "a single domain in a single grain" in a polycrystalline aggregate could be achieved.

In this study, the dependence of the dielectric properties on the average grain size down to a few tens of nanometer range in dense PMN-30PT ceramics has been investigated. In particular, we explored the possibility of achieving a system with intrinsic stresses, which is expected to impede the temperature-dependent transformation from the rhombohedral to tetragonal phase and elevate T_C by increasing the coercivity. For that purpose, the nanostructured powders prepared from a blend of elemental oxides by high energy ball milling were compacted by means of the spark plasma sintering (SPS) technique, which is known to be especially attractive for the densification of nanostructured powders with minimal grain growth.[27–30] Thereafter, appropriate heating conditions were chosen to vary the grain size of the consolidated specimens. The phase analysis and dielectric property measurements on these specimens with different grain size revealed several novel features of this material.

II. EXPERIMENTAL PROCEDURE

Powders of PbO (>99.9% purity, Aldrich Chemical Co., Milwaukee, WI), TiO_2 (>99.9% purity, Aldrich Chemical Co., Milwaukee, WI), Nb_2O_5 (>99.9% purity, Aldrich Chemical Co., Milwaukee, WI), and MgO (>99.9% purity, High Purity Chemical Co., Saitama, Japan) of about 50–100 μm particle size were blended in appropriate proportions conforming to the composition of PMN-30PT and 1 wt % excess PbO was added to compensate for the PbO loss during sintering. Then, the powder blends were ball milled at a mill speed of 250 rpm in a planetary ball mill (Fritsch Pulverisette 5, Germany), with wet medium (toluene). WC balls were used as a grinding media and the weight ratio of the balls to powder was set to be 10:1. The milling was performed for 10, 20, or 40 h without stopping with a view to promoting the formation of nanocrystals[7,31] and synthesizing PMN-30PT. The evolution of phases and their crystallite size were monitored by x-ray diffraction (XRD) technique (Cu $K\alpha$) (D8 Advanced, Bruker Co., Germany). A transmission electron microscope (TEM) (JEM 3000F, JEOL, Japan) was used to verify the crystallite sizes estimated by XRD.

The as-milled powders were placed in a graphite die (10 mm in diameter) and heat treated at 750 °C for 5 min under vacuum of 2.7 Pa in a SPS furnace (ElTek Co., Korea). The pressure and electric current applied during sintering were 30 MPa and 1200 A, respectively. This sintering condition was chosen on the basis of preliminary experiments. Then, the SPSed samples were heated at a rate of 5 °C/min to a predetermined annealing temperature. The specimens were annealed at 650 °C for 30 min (*S* specimen), at 800 °C for 1 h (*M* specimen), 1000 °C for 8 h (*ML* specimen), and 1200 °C for 10 h (*L* specimen) in order to vary the average crystallite size in the final products. During this treatment the specimens were placed in a tightly sealed platinum crucible under the cover of a mixture of $PbZrO_3$-5 wt % PbO powder to minimize the PbO evaporation from the specimen.

The microstructures of the sintered products were characterized by TEM and scanning electron microscope (SEM) (JSM-6330F, JEOL, Japan). The average grain size of each sintered product was obtained from the mean intercept length multiplied by a geometric proportionality constant (e.g., for the *L*, *ML*, *M* specimens: 1.775 and for the *S* specimen: 1.5).[32] An ultraslow scan of the {200} peak in the XRD, at the speed of 0.00274 deg/s, was performed to track the phase formation in each specimen. The dielectric properties of each specimen were measured by means of an impedance analyzer (model HP 4194A, Hewlett-Packard, Tokyo, Japan) and the density was determined by the Archimedes method.

III. RESULTS

Figure 1(a) shows the modulation in the XRD patterns of the as-milled powder with the progress of ball milling. Here, after 20 h milling the characteristic peaks of PMN-30PT, such as (100), (110), and (200), are clearly discernable. Further milling up to 40 h showed no significant change in the XRD pattern except some peak broadening, which indicates the formation of nanostructured phases. The double-Voigt method[33,34] revealed the average crystallite size in the 20 and 40 h-milled powder to be about 20 and 10 nm, respectively. These values were in good agreement with the TEM micrograph in Fig. 1(b).

The as-milled powder was SPSed at 750 °C for 5 min. The XRD pattern in Fig. 2(a) revealed that the sintered prod-

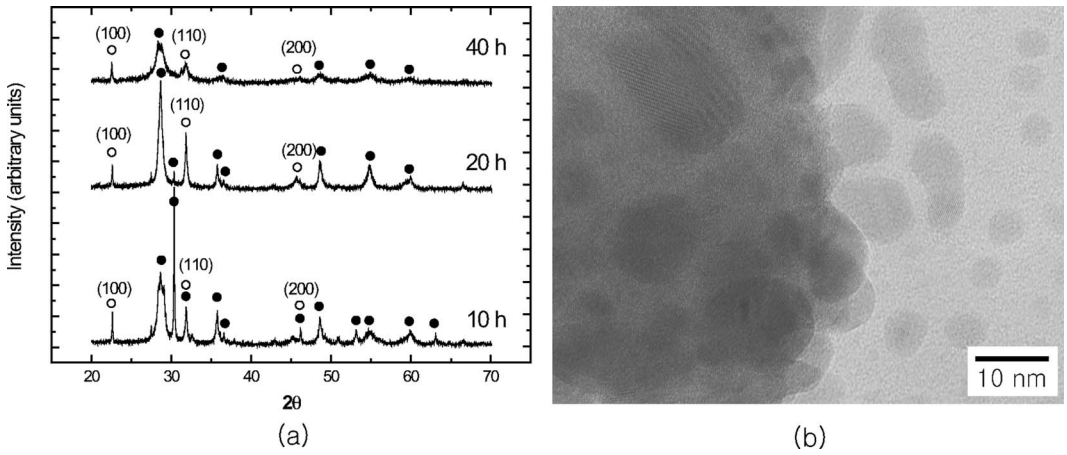

FIG. 1. (a) XRD pattern of the as-milled powders: (●) PbO and (◯) PMN-30PT. Here XRD line broadening with the progress of milling indicates the formation of nanocrystals. (b) TEM image of the 40 h milled powder confirms the formation of nanocrystals.

uct at this stage was mostly composed of three phases, namely, the PMN-30PT perovskite phase, the $Pb_2Mg_xNb_{1.33}O_{5.33+x}$ (for $0<x<0.66$) pyrochlore phase, and PbO. The relative amount of the perovskite and pyrochlore phase, obtained from the intensity ratios of (110) peaks from these phases, while neglecting the presence of PbO, was estimated to be 34% and 66%, respectively. The bright-field TEM image in Fig. 2(b) evidences that the SPSed specimen had a grain size of about 50 nm.

The $Pb_2Mg_xNb_{1.33}O_{5.33+x}$ phase detected in the SPSed sample is known as a *B*-site (Nb) deficient pyrochlore phase, which transforms into a single phase perovskite during heating,[35,36] while the commonly referred pyrochlore phase, $Pb_{1.83}Nb_{1.71}Mg_{0.29}O_{6.37}$ (*A* site, i.e., Mg deficient pyrochlore phase) persists, once formed.[37] The formation of the *B*-site deficient pyrochlore phase during the high energy ball milling process may be attributed to a different dissolution rate of MgO and Nb_2O_5 in PbO, since MgO is usually expected to dissolve more easily than Nb_2O_5 during the milling process. In other words, the reactivity of MgO might be high enough to enhance the formation of *B*-site deficient pyrochlore phase with PbO even in the presence of Nb_2O_5.[36]

In order to vary the grain size of the SPSed products, four sets of the annealing condition in air were used to generate the *S*, *M*, *ML*, and *L* specimens (cf. Sec. II). Complete formation of the perovskite-phase PMN-30PT in all the four specimens was confirmed from the XRD patterns in Fig. 3. It shows that the pre-existing *B*-site deficient pyrochlore phase in the SPSed product was converted completely to the perovskite phase during the annealing process. The ultraslow scan of the {200} XRD peak (cf. Sec. II) of each specimen revealed the presence of the perovskite cubic phase alone in the *S* specimen, a coexistence of cubic and rhombohedral phases in the *M* specimen, and a coexistence of rhombohedral and tetragonal phases in the *ML* and *L* specimens. The detailed crystallographic information on the {200} peak of each specimen has been summarized in Table I.

Figure 4 illustrates the fractured surface of the *S*, *M*, *ML*, and *L* specimens, as observed by SEM. These micrographs clearly evidence the effectiveness of the prior SPS condition in obtaining fully dense specimens. It can be noticed that the unimodal grain-size distribution of *S* [see Fig. 4(a)] changes into bimodal one in the *M* [see Fig. 4(b)] and *ML* specimens [see Fig. 4(c)], and finally evolves into a unimodal one in the *L* specimen [see Fig. 4(d)] again. The average grain size of each of these four samples, determined by the mean intercept method,[32] was found to be about 91, 334

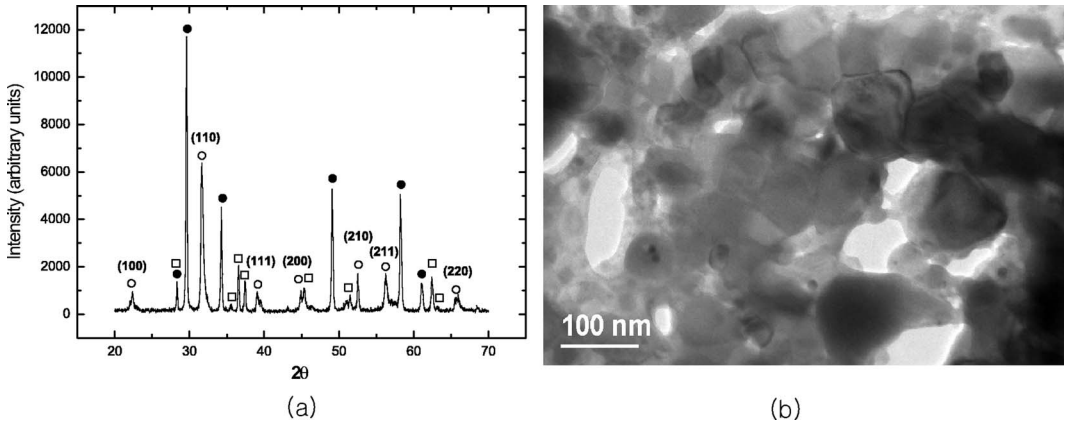

FIG. 2. (a) XRD pattern of the SPSed sample: (◯)PMN-30PT perovskite, (●) $Pb_2Mg_xNb_{1.33}O_{5.33+x}$ pyrochlore phase, and (□) PbO. (b) TEM micrograph of the SPSed specimen evidences a complete densification and nanocrystallization (~50 nm) of the grains.

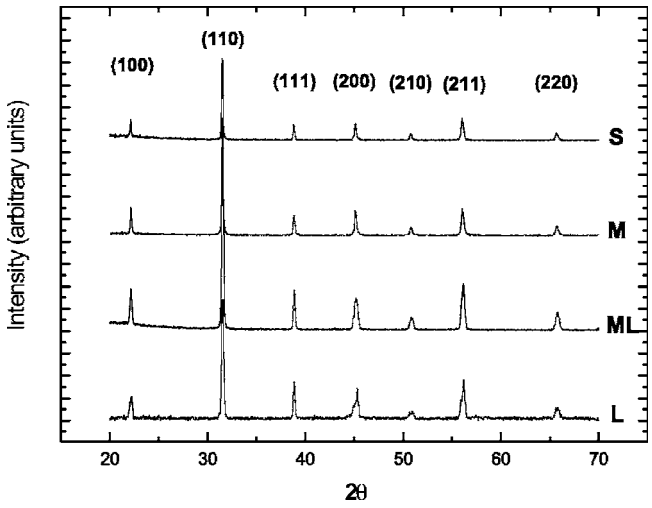

FIG. 3. XRD pattern of the *S*, *M*, *ML*, and *L* specimens, confirming the complete formation of perovskite-structured PMN-30PT.

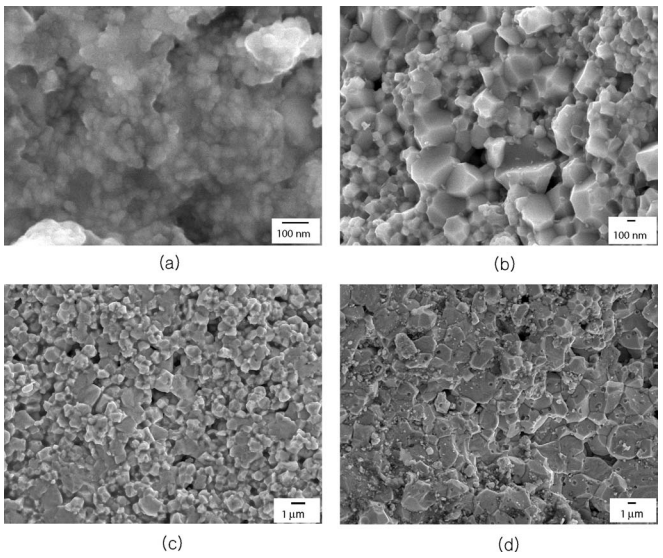

FIG. 4. (a), (b), (c), and (d) show the SEM fractograph of the *S*, *M*, *ML*, and *L* specimens, respectively. Note that the *M* and *ML* specimens show bimodal size distribution, while the *S* and *L* specimens exhibit relatively uniform size distribution.

nm (bimodal distribution of 280 and 690 nm), 1.8 μm (bimodal distribution of 1.1 μm and 2.2 μm), and 5.7 μm, respectively.

The measured dielectric constant and corresponding dielectric loss tangent for each specimen at the frequency of 1 kHz are shown in Figs. 5(a) and 5(b) and those measured at 1 MHz are given in Figs. 5(c) and 5(d), respectively. At 1 kHz, where the space charge contribution prevails, it was observed that the maximum dielectric constant tends to decrease but that of tail regions at both high and low temperatures increases with the reduction in the average grain size up to that of the *M* specimen. Note that a convex shape with an apparent dielectric maximum was no longer observed in the *S* specimen, which indicates that the *S* specimen may be classified to the paraelectric category. The dielectric loss of the *L* specimen shown in Fig. 5(b) exhibits a clear peak at about 95 °C and a certain fluctuation at about 170 °C. The former can be attributed to the transformation from rhombohedral to tetragonal structure, while the latter one evidences the conversion from the tetragonal to cubic phase.[3]

On the other hand, at 1 MHz, where the space charge contribution could be ignored, a reduction in the overall dielectric constant of all the four specimens was observed [Fig. 5(c)]. In this case, the high level of dielectric constant that existed near the tail region of the plots for the *ML* specimen at 1 kHz [Fig. 5(a)], decreased significantly. In contrast, the *M* specimen still showed almost a temperature-independent high dielectric constant. The dielectric loss tangent of the *ML*, *M*, and *S* specimens measured at 1 MHz showed that the divergence in the dielectric constant spectra in Fig. 5(c) from that in Fig. 5(a) should be related to the mechanism operating at a higher frequency because then the space charge contribution becomes insignificant. All the properties of the present PMN-30PT specimens measured in these experiments are summarized in Table II.

TABLE I. Crystallographic information obtained from the detailed analysis on the {200} peak.

	d spacing (nm)	(*hkl*)	Phase[a]	Ω (10^{-2} nm^3)
S	0.20169	(200)	*C*	6.5636
M	0.20146	(200)	*R* (30%)	6.5404
	0.20135	(200)	*C*	6.5305
ML	0.20274	(002)	*T*	6.5208
	0.20140	(200)	*R* (70%)	6.5346
	0.20051	(200)	*T*	
L	0.20204	(002)	*T*	6.4854
	0.20105	(200)	*R* (67%)	6.5006
	0.20031	(200)	*T*	

[a]*C*, *R*, and *T* represent cubic, rhombohedral, and tetragonal, respectively.

IV. DISCUSSION

A. Size-driven phase transformation

The phases observed at each stage of the present experiments on the bulk specimens can be summarized as follows:

(1) 34% cubic perovskite PMN-30PT and 66% pyrochlore $Pb_2Mg_xNb_{1.33}O_{5.33+x}$ phase of the average grain size of 50 nm in the SPSed specimen (when the residual PbO content is ignored);
(2) 100% cubic perovskite PMN-30PT in the *S* specimen with the average grain size of 91 nm;
(3) 70% cubic and 30% rhombohedral PMN-30PT in the *M* specimen having the average grain size of 334 nm (a mixture of 280 and 690 nm);
(4) 70% rhombohedral and 30% tetragonal PMN-30PT in the *ML* specimen showing the average grain size of 1.8 μm (a mixture of 1.1 and 2.2 μm); and
(5) 67% rhombohedral and 33% tetragonal PMN-30PT in the *L* specimen with the average grain size of 5.7 μm.

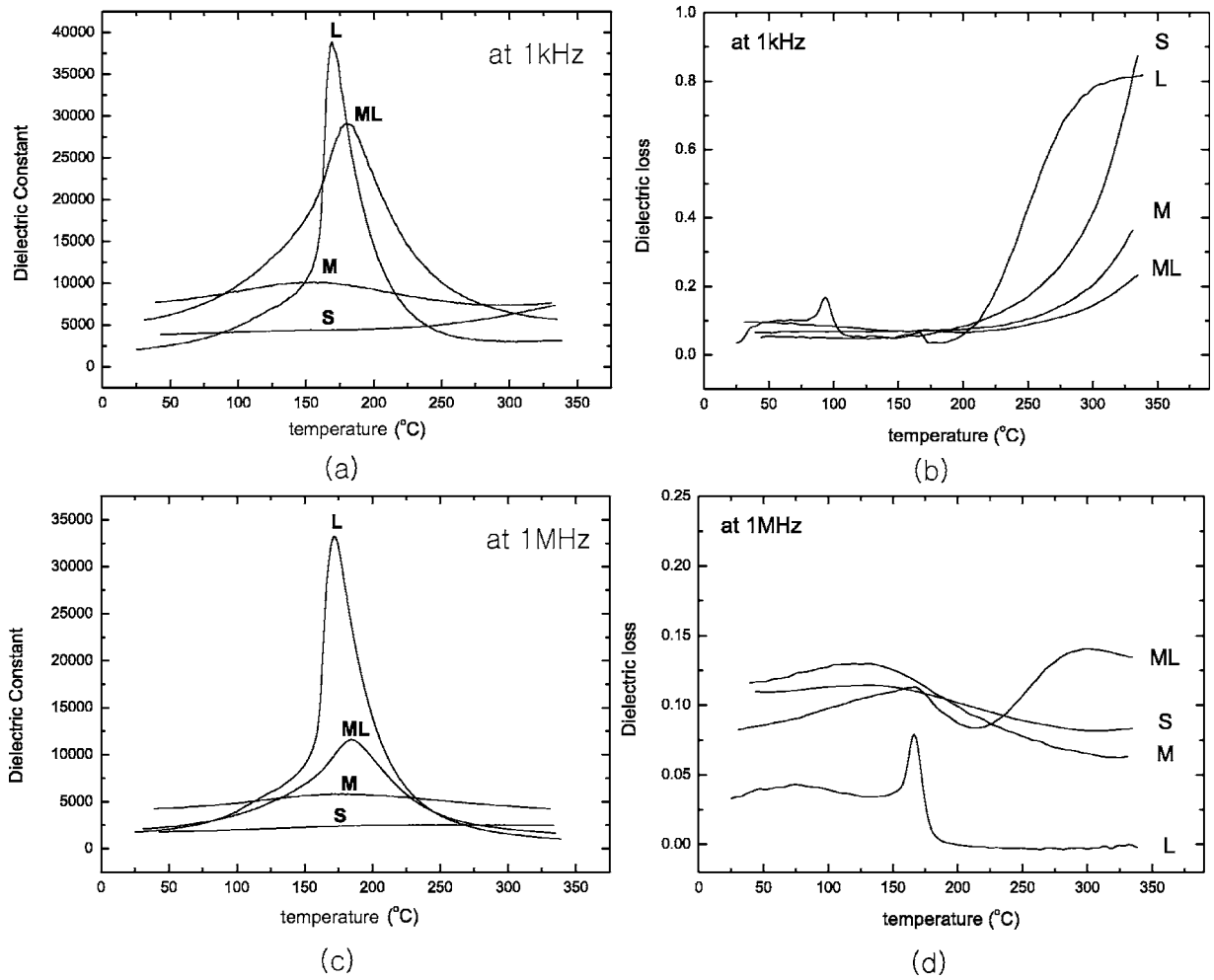

FIG. 5. Temperature dependence of dielectric constants and corresponding dielectric loss of the *L*, *ML*, *M*, and *S* specimens at the frequency of 1 kHz [(a) and (b)] and 1 MHz [(c) and (d)], respectively.

It is obvious from these observations that the cubic phase of PMN-30PT is stable against the phase transformation at least up to about 90 nm in the average grain size. It can also be noted from the present experiments that the conventional transformation of the cubic perovskite phase in PMN-30PT existing at the sintering temperature into the tetragonal phase during cooling process seems to be suppressed in the system with the grain size of <690 nm, and the percentage of the rhombohedral phase increases from 30% to maximum 70% as the average grain size of PMN-30PT increases from 334 nm to 1.8 μm. A conversion of the cubic phase into a mixture of the rhombohedral and tetragonal phase at MPB occurs at >700 nm in size.

TABLE II. Measured properties of PMN-30PT in each condition.

	Grain size (nm)	Density (%)	T_m [a] (°C)	ε_m (1 kHz)
S	91	98.6	N/A[b]	N/A
M	334	98.5	156	10144
ML	1400	95.2	180	29093
L	5700	93.9	169	38859

[a] T_m represents the temperature for the maximum dielectric constant.
[b] N/A stands for "not applicable."

It is obvious that the high temperature paraelectric cubic phase is stabilized at the room temperature in the *S* specimen, since a size refinement commonly results in the reduction of the equilibrium temperature between a high and low temperature polymorph due to the capillary effect.[38] As a matter of course, this has been clearly demonstrated experimentally in various ferroelectric materials.[10–13,17–19,39] However, the capillary-based mechanism does not seem to be enough to explain the predominance of rhombohedral phase over tetragonal in the *M* specimen because the cubic phase is expected to change not to the rhombohedral but to the tetragonal phase as the capillarity effect decreases.[3]

In a recent study of the grain-size effects on the ferroelectric behavior of dense nanocrystalline $BaTiO_3$ ceramics, Zhao *et al.*[12] strongly indicated that the usually observed size-driven effect in ferroelectric materials comes not only from the intrinsic effect which is related to the capillary or Landau–Ginsburg–Devonshire theory but also from the extrinsic effect like from the grain boundaries. Besides, they noted that the measurements of the dielectric properties alone cannot provide conclusive evidence about the origin of the size effects in ceramics. It follows that the interpretation of the size effect on the phase transformation in the present PMN-30PT also needs to consider the extrinsic effect.

A close look at the data in Table I in conjunction with the crystal size of the specimens reveals the following interesting features:

(1) The unit cell size of each phase increased with the reduction in crystal size. For the cubic phase it increased from 6.5305×10^2 nm^3 in the *M* specimen to 6.5636×10^2 nm^3 in the *S* specimen. It shows that with the reduction in crystal size in bulk specimen there is an expansion in the lattice. This phenomenon is quite common in several metallic systems like Nb,[40] Nb-Al,[41] Ni-Si,[42] and W.[43] The origin of this effect can be attributed to the NHP exerted on the crystals by the free volume at the grain boundaries.[6,7] It is also apparent that the surface bond contraction due to the reduction in the ionic radius on the surface[8,9] which would otherwise cause a reduction in the unit cell volume, does not play any significant role in the present nanostructured bulk specimens.

(2) In any given specimen at room temperature, the unit cell size of rhombohedral phase > cubic phase > tetragonal phase. It appears that at a small grain size, as in the *S* specimen, the NHP is high enough to prevent the high-temperature cubic phase from transforming to a phase with a lower symmetry during cooling process. However, as the grain size of specimens increases, the level of the NHP, which causes a shrinkage of the lattice of cubic phase, decreases so rapidly that the formation of rhombohedral phase with larger specific volume compared to that of tetragonal phase (in any given specimen) appears promoted. Further reduction in the NHP with the increase in the grain size seems to manifest a reduction in the specific volume of rhombohedral phase and trigger the formation of tetragonal phase.

In summary, the dependence of the sequence of phase formation in the present PMN-30PT ceramics on the grain size can be qualitatively explained on the basis of capillary effect and the NHP originating from the presence of a free volume at the grain boundaries.

B. Dielectric behavior

The measured values of the dielectric constant of each specimen, shown in Figs. 5(a) and 5(c), depict a drastic decrease in the maximum dielectric constant during size reduction, which is in conformity with the results in the literature.[21–24] The reduction in the dielectric constant of the *ML* and *M* specimens compared with the *L* specimen has been attributed to the increased proportion of highly insulating grain boundaries[21–23] and the diffused ferroelectric-to-paraelectric transition to a destruction of the ferroelectric domain state toward polar nanoregions in a paraelectric matrix.[24] However, this mechanism seems to be insufficient to explain the increase in T_m of the *ML* specimen and the nearly constant dielectric property of the *M* specimen over a wide range of measuring temperature even at a high frequency of 1 MHz. A plausible explanation of these observations can be put forward as follows.

One of the most important features defining a ferroelectric relaxor is a dielectric dispersion with temperature and frequency.[23] Both the *ML* and *M* specimens show a dispersion in the dielectric constant, but the frequency dependent dispersion was observed to be marginal in the *ML* specimen, as is evident from Fig. 6(a). The degree of dispersion for the *ML* and *M* specimens between 1 kHz and 1 MHz is estimated to be 0.02 and 0.15, respectively. Consequently, eliminating the space charge effect due to the increase in the grain boundary area, the *ML* specimen may not be classified as a relaxor, but rather as a normal ferroelectrics of the MPB composition with a wide range of grain size distribution, which may lead to a spectrum of T_C. It follows that the relaxor behavior observed in the *ML* specimen is thought to be a mixture of those of a relaxor and a normal ferroelectrics, as was discussed by Diamond[44] and Martirena and Burfoot.[20] Moreover, the increase in the T_m can be attributed to the increase in the spontaneous polarization (P_S), which results in the increase of T_C of the tetragonal phase.

On the other hand, the dielectric constant values shown in Fig. 6(c) show that the *M* specimen could be classified as a relaxor, although the tendency is rather weak. This may be attributed to a high fraction of the paraelectric cubic phase. Note that the increase in the dielectric constant above 300 °C may be caused by the presence of ~70% of cubic phase (see Table I). In addition, Fig. 6(d) indicates that the origin of the temperature-insensitive high dielectric constant of the *M* specimen may not be from the space charge contribution, since the dielectric loss tangent spectrum at 1 kHz is similar to that of paraelectric materials; but the difference from the paraelectric behavior becomes evident as the frequency increases [see Figs. 5(b) and 5(d)].

One possible explanation of the relatively high but nearly invariable dielectric constant of the *M* specimen over the entire range of the measuring temperature can be found from the analogy to the superparamagnetic theory. According to the theory on superparamagnetics, there should exist a state of a single domain in a single grain, right before the superparamagnetic state is induced, and the coercivity is known to reach its maximum value at that state.[26] Considering the similarity between the ferromagnetic and the ferroelectric phenomena, the state of a single domain in a single grain is expected to exist at a certain size level in ferroelectric materials, too; and at that state an increase in the coercivity, which resists the thermal randomizing effect, could greatly enhance the dielectric constant both at low and high temperature region.

Furthermore, the absence of the domain wall would also prevent the domain from being switched easily. Note the domain wall provides a preferential nucleation site for a ferroelectric domain of the opposite direction.[45] In summary, the concept of the state of the single domain in a single grain with a high coercivity can explain why the diffuse dielectric property is gradually flattened, especially in the *M* specimen which contains 70% cubic phase, and why the dielectric constant data both at low and high temperature regions significantly increase to make the dielectric behavior of the system insensitive to the temperature change.

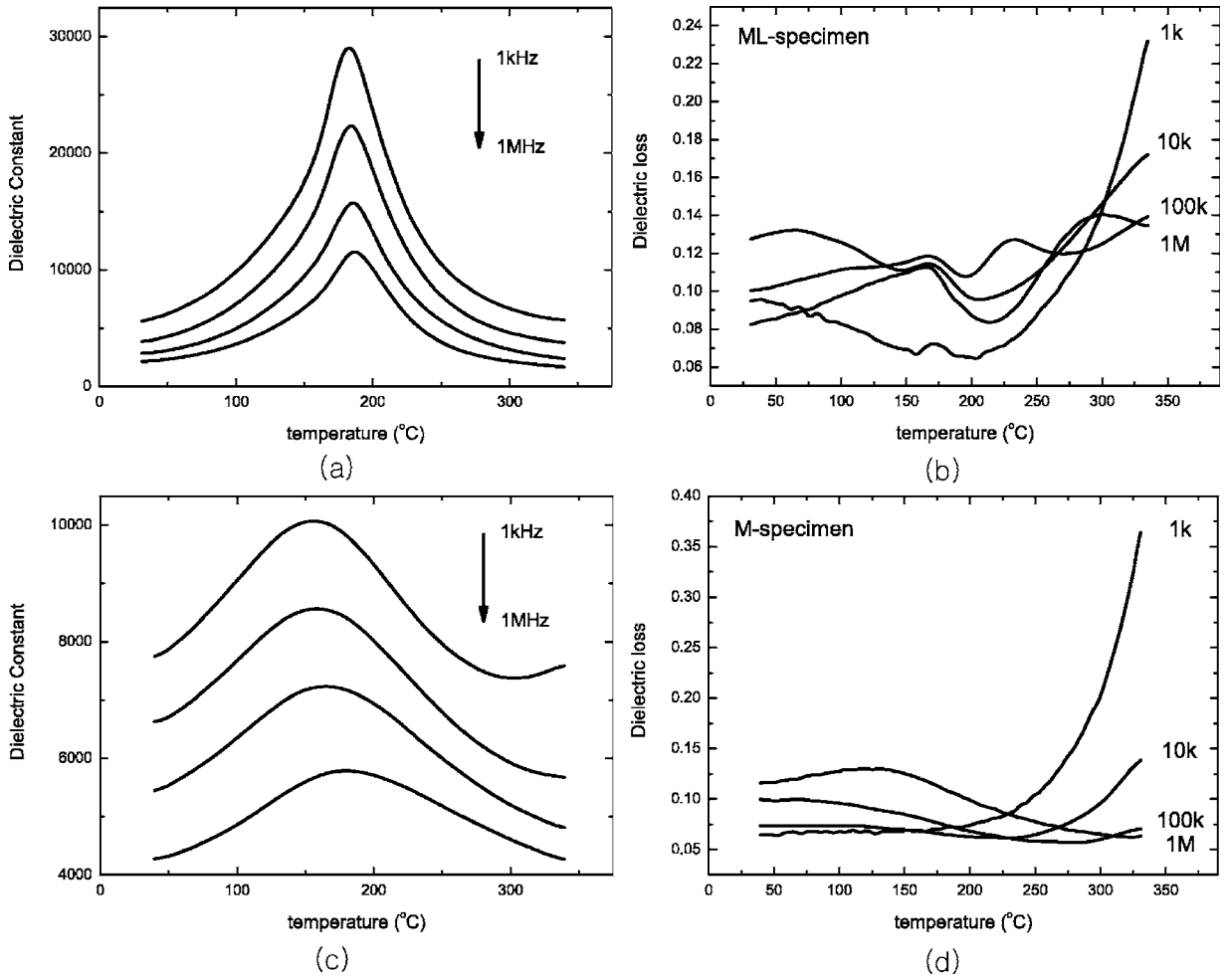

FIG. 6. Frequency dependence of dielectric constant and corresponding dielectric loss at 1, 10, 100 kHz, and 1 MHz of (a) and (b) the *ML* specimen and (c) and (d) the *M* specimen. Note that the *M* specimen shows a relaxor behavior with dielectric dispersion as a function of temperature and frequency, while the *ML* specimen exhibits a relaxor behavior since it lacks in the dielectric dispersion with respect to frequency.

V. CONCLUSION

The effect of the grain size on the phase transformation and dielectric properties of PMN-30PT was investigated. A high-temperature cubic phase formed during sintering was observed to remain stable at the room temperature when the average crystal size reached down to ~90 nm. The increase in the average grain size was noticed to trigger the formation of the rhombohedral phase and then the tetragonal phase. The evolution of the crystal structure of PMN-30PT with the grain size was qualitatively explained on the basis of the capillary effect and the negative hydrostatic pressure exerted on the crystal by the free volume at the grain boundaries.

The maximum dielectric constant value was observed to decrease with grain size refinement possibly due to the increase in the total grain boundary area, and a relaxor behavior appeared as the crystallite size decreased. At a certain level of the grain size (in the *M* specimen), however, the observed anomalous behavior of the dielectric constant, i.e., a relatively high dielectric constant over the entire range of measuring temperature (30–330 °C), was attributed to the possible contribution of the specific state of a single domain in a single grain, which may enhance the coercivity. Further refinement in the average grain size down to ~90 nm manifested a paraelectric transition, and the phenomenon was explained in terms of the size-driven phase transformation.

ACKNOWLEDGMENTS

This work was supported by the Ministry of Education and Human Resources Development of the Korean Government through the Brain Korea 21 Project. S.K.P. acknowledges the financial support of the Seoul National University, Korea for his stay there.

[1]S. E. Park and T. R. Shrout, J. Appl. Phys. **82**, 1804 (1997).
[2]H. Fu and R. E. Cohen, Nature (London) **403**, 281 (2000).
[3]S. W. Choi, T. R. Shrout, S. J. Jang, and A. S. Bhalla, Mater. Lett. **8**, 253 (1989).
[4]R. E. Eitel, C. A. Randall, T. R. Shrout, and S.-E. Park, Jpn. J. Appl. Phys., Part 1 **41**, 2099 (2002).
[5]N. J. Ramer, S. P. Lewis, E. J. Mele, and A. M. Rappe, in *First Principles Calculations for Ferroelectrics*, Fifth Williamsburg Workshop, edited by R. E. Cohen (AIP, Woodbury, 1998), p. 156.
[6]H. J. Fecht, Acta Metall. Mater. **38**, 1927 (1990).
[7]P. P. Chattopadhyay, P. M. G. Nambissan, S. K. Pabi, and I. Manna, Phys. Rev. B **63**, 054107 (2001).
[8]H. Huang, C. Q. Sun, and P. Hing, J. Phys.: Condens. Matter **12**, L127 (2000).
[9]H. Huang, C. Q. Sun, Z. Tianshu, and P. Hing, Phys. Rev. B **63**, 184112 (2001).

[10]K. Uchino, E. Sadanaga, and T. Hirose, J. Am. Ceram. Soc. **72**, 1555 (1989).
[11]M. P. McNeal, S.-J. Jang, and R. E. Newham, J. Appl. Phys. **83**, 3288 (1998).
[12]Z. Zhao, V. Buscaglia, M. Viviani, M. T. Buscaglia, L. Mitaseriu, A. Testino, M. Nygren, M. Johnsson, and P. Nanni, Phys. Rev. B **70**, 024107 (2004).
[13]W. L. Zhong, Y. G. Wang, P. L. Zhang, and B. D. Qu, Phys. Rev. B **50**, 698 (1994).
[14]C. J. Lu, S. B. Ren, H. M. Shen, J. S. Liu, and Y. N. Wang, J. Phys.: Condens. Matter **8**, 8011 (1996).
[15]Z. Ye, E. B. Slamovich, and A. H. King, J. Mater. Res. **20**, 558 (2005).
[16]S. Chattopadhyay, P. Ayyub, V. R. Palkar, and M. Multani, Phys. Rev. B **52**, 13177 (1995).
[17]B. Jiang, J. L. Peng, L. A. Bursill, and W. L. Zhong, J. Appl. Phys. **87**, 3462 (2000).
[18]L. Zhang, W. L. Zhong, C. L. Wang, Y. P. Peng, and Y. G. Wang, Eur. Phys. J. B **11**, 565 (1999).
[19]Y. L. Du, M. S. Zhang, Q. Chen, and Z. Yin, Appl. Phys. A: Mater. Sci. Process. **76**, 1099 (2003).
[20]H. T. Martirena and J. C. Burfoot, J. Phys. C **7**, 3182 (1974).
[21]T. R. Shrout, U. Kumar, M. Megherhi, N. Yang, and S.-J. Jang, Ferroelectrics **76**, 479 (1987).
[22]P. Papet, J. P. Dougherty, and T. R. Shrout, J. Mater. Res. **5**, 2902 (1990).
[23]L. E. Cross, Ferroelectrics **76**, 241 (1987).
[24]J. Carreaud, P. Gemeiner, J. M. Kiat, B. Dkhil, C. Bogicevic, T. Rojac, and B. Malic, Phys. Rev. B **72**, 174115 (2005).
[25]J. R. Groza, in *Nanostructured Materials-Processing, Properties and Potential Applications*, edited by C. C. Koch (Noyes, New York, 2002), pp. 115–178.
[26]B. D. Cullity, *Introduction to Magnetic Materials* (Addison-Wesley, Reading, MA, 1972).
[27]J.-K. Park, U.-J. Chung, N. M. Hwang, and D.-Y. Kim, J. Am. Ceram. Soc. **84**, 3057 (2001).
[28]E. M. Perera, M. Tokita, and S. Morricca, J. Eur. Ceram. Soc. **18**, 401 (1998).
[29]E. M. Carrillo-Heian, C. Unuvar, J. C. Gibeling, G. H. Paulino, and Z. A. Munir, Scr. Mater. **45**, 405 (2001).
[30]J. Hong, L. Gao, S. D. D. L. Torre, H. Miyamoto, and K. Miyamoto, Mater. Lett. **43**, 27 (2000).
[31]J. Xue, J. Wang, and T. M. Rao, J. Am. Ceram. Soc. **84**, 660 (2001).
[32]J.-H. Han and D.-Y. Kim, Acta Metall. Mater. **43**, 3185 (1995).
[33]T. H. de Keijser, J. I. Langford, E. J. Mittemeijer, and A. B. P. Vogels, J. Appl. Crystallogr. **15**, 308 (1982).
[34]D. Balzar, in *Defect and Microstructure Analysis from Diffraction*, International Union of Crystallography Monographs on Crystallography No. 10, edited by R. L. Snyder, H. J. Bunge, and J. Fiala (Oxford University Press, New York, 1999), p. 94.
[35]F. Chaput, J. P. Boilot, M. Lejeune, R. Papiernik, and L. G. Hubert-Pfalzgraf, J. Am. Ceram. Soc. **72**, 1355 (1989).
[36]K. R. Han, H. J. Koo, and C. S. Lim, J. Am. Ceram. Soc. **83**, 2214 (2000).
[37]S. L. Swartz and T. R. Shrout, Mater. Res. Bull. **17**, 1245 (1982).
[38]C. X. Wang and G. W. Yang, Mater. Sci. Eng., R. **49**, 157 (2005), and references therein.
[39]J. Zhang, Z. Yin, M.-S. Zhang, and J. F. Scott, Solid State Commun. **118**, 241 (2001).
[40]P. P. Chattopadhyay, S. K. Pabi, and I. Manna, Mater. Sci. Eng., A **304–306**, 424 (2001).
[41]P. P. Chatterjee, S. K. Pabi, and I. Manna, J. Appl. Phys. **86**, 5912 (1999).
[42]M. K. Datta, S. K. Pabi, and B. S. Murty, J. Appl. Phys. **87**, 8393 (2000).
[43]R. Malewar, K. S. Kumar, B. S. Murty, B. Sarma, and S. K. Pabi, J. Mater. Res. **22**, 1200 (2007).
[44]H. Diamond, J. Appl. Phys. **32**, 909 (1961).
[45]W. J. Merz, Phys. Rev. **95**, 690 (1954).